Anal Bioanal Chem (2004) 378 : 1608–1615
DOI 10.1007/s00216-004-2504-6

PAPER IN FOREFRONT

Daniel Kang · Dulasiri Amarasiriwardena
Alan H. Goodman

Application of laser ablation–inductively coupled plasma-mass spectrometry (LA–ICP–MS) to investigate trace metal spatial distributions in human tooth enamel and dentine growth layers and pulp

Received: 5 October 2003 / Revised: 21 December 2003 / Accepted: 12 January 2004 / Published online: 5 February 2004

Abstract Human tooth enamel provides a nearly permanent and chronological record of an individual's nutritional status and anthropogenic trace metal exposure during development; it might thus provide an excellent bio archive. We investigated the micro-spatial distribution of trace metals (Cu, Fe, Mg, Sr, Pb, and Zn) in 196×339 μm^2 raster pattern areas (6.6×10^4 μm^2) in a deciduous tooth using laser ablation-inductively coupled plasma-mass spectrometry (LA–ICP–MS). Ablated areas include prenatal and postnatal enamel, the neonatal line, the dentine–enamel junction (DEJ), dentine, and the dentine–pulp junction. Topographic variations in the surface elemental distribution of lead, zinc, strontium, and iron intensities in a deciduous tooth revealed heterogeneous distribution within and among regions. ^{43}Ca normalized elemental intensities showed the following order: Sr>Mg>>Zn>Pb>Fe>Cu. Elevated zinc and lead levels were present in the dental pulp region and at the neonatal line. This study demonstrates the ability of LA–ICP–MS to provide unique elemental distribution information in micro spatial areas of dental hard tissues. Elemental distribution plots could be useful in decoding nutrition and pollution information embedded in their bio apatite structure.

Keywords Human teeth · Trace metals · Enamel growth layers · Micro spatial distribution · Laser ablation–inductively coupled plasma–mass spectrometry (LA–ICP–MS)

Presented in part at the 2002 Winter Conference on Plasma Spectrochemistry, Scottsdale, AZ, January 6–12, 2002. The poster was selected as an outstanding poster presentation.

D. Kang · D. Amarasiriwardena (✉) · A. H. Goodman
School of Natural Science,
Hampshire College,
Amherst, MA 01002, USA
e-mail: dula@hampshire.edu

Introduction

Teeth, and especially dental enamel, reflect past metabolic, nutritional, and pollution events [1, 2, 3, 4, 5]. Enamel develops and calcifies in a highly controlled, regular, and ring-like manner, and once formed is not subjected to mineral resorption. In addition to enamel, human teeth comprise two additional and distinct tissue layers: dentine comprises the bulk of a tooth and cementum is located on the outer surfaces of tooth roots (Fig. 1). Mature enamel contains no active cells and is approximately 97% inorganic. Mature dentine and cementum, are also highly calcified and nearly inert, although less so than enamel. In addition, after initial calcification, zones of secondary dentine and cementum may form [6].

Bioapatite crystal formation is under direct metabolic and physiological control of the organism, and thus trace

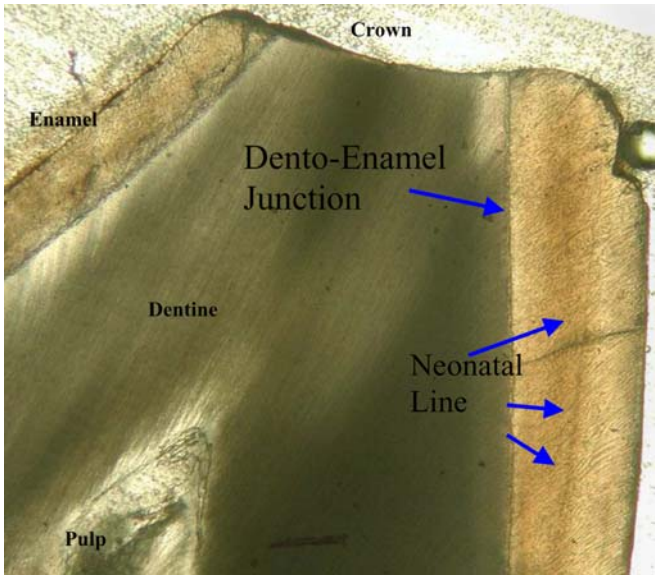

Fig. 1 Enamel, dental, and pulp tissue regions of a deciduous tooth obtained by thin section optical microscopy

metal signatures, their chemistry, and concentrations within the bioapatite reflect the load and status of the metabolism of trace metals [7]. Enamel and dentine are predominately composed of hydroxyapatite ($Ca_3(PO_4)_5OH$) crystals. Hexagonal hydroxyapatite crystals in enamel are bundled to form approximately 4 µm diameter rods, which occupy a position at nearly right angles to the tooth surface [8]. In addition to enamel's prominent inorganic matrix, the organic constituents (i.e., proteins and lipids) and water (4% *w*/*w*) occupy space between the apatite crystals in the enamel. The calcium and phosphorus (as phosphate) content of teeth range from 34 to 39% and 16–18% by weight, respectively [8]. Enamel is composed of regular incremental growth layers where various cations and anions are incorporated into cationic (Ca^{2+}) and anionic centers (OH^-, PO_4^{3-}) of the hydroxyapatite matrix. Major cations Na^+, K^+, and Mg^{2+} and anions CO_3^{2-}, F^-, and Cl^- are present in enamel as major substituted species. Close to 40 elements have been reported to be present in the ≥1000 ppm (i.e., Zn, Sr, Fe, Al, B, Ba, Pb ...) to ≤100 ppb (i.e., Ni, Li, Ag, As, Se, Nb, Hg ...) range [8].

Deciduous tooth enamel commences calcification at the end of the first trimester in utero and continues to develop up to a year after birth. Dentine begins formation at the same time but continues to calcify to around two and a half years of age [3]. In contrast, permanent tooth enamel and dentine begin calcification around birth and, in the case of the third molar, continue to calcify into adolescence. Physiological perturbations and nutritional and environmental changes can permanently alter both the amount of enamel that is laid down and its chemistry. In some cases distinct areas of hyper or hypo mineralization can be observed on teeth [3, 9]. In the worst cases particularly with exposure to elevated levels of fluoride [10] or lead, dark mottled regions are seen.

Enamel growth layers look similar to those of an onion or artichoke in that the layers deepest and closest to the dentine and at the tip or occlusal end of the tooth grow first and subsequent layers cover the first developing layers and continue to grow down the sides of tooth crowns. Unique trace elemental signatures are embedded in those calcified enamel layers, and thus they can act as an excellent chemical archive to monitor past elemental variations owing to nutritional changes and pollution events during prenatal and postnatal development. The pattern of deposition and intensity of nutritionally and toxicologically important elements in enamel layers can provide clues to past nutrition and pollution-related episodes.

Trace metal concentrations in teeth are most often determined by bulk techniques in which whole teeth or some portion of enamel or dentine is digested in a suitable mineral acid [2]. Among the analytical methods, flame atomic absorption spectroscopy (FASS), inductively coupled plasma emission (ICP–AES) and mass spectrometry (MS), neutron activation analysis (NAA), and anodic striping voltammetry (ASV) are commonly used to measure trace elemental content in the digested teeth [2]. Unfortunately, bulk analyses of dental tissue destroy the time-based elemental distribution profiles.

In laser ablation-inductively coupled plasma-mass spectrometry (LA–ICP–MS), a high-energy pulsed laser beam is directed on to predetermined surface location of a tooth sample placed in an enclosed sampling chamber. The interaction of the laser beam energy with the solid sample produces an ablated micro sample in the vapor phase. The vaporized sample is transported by a stream of argon gas into the plasma region where the high temperature of the discharge produces predominately singly charged atomic ions, which are then extracted into the mass spectrometer for detection. High sensitivity, low detection limits, along with depth profiling and surface area scanning makes LA–ICP–MS an attractive technique for analysis of the spatial distribution of elements [11, 12, 13, 14].

For example, LA–ICP–MS has been used to determine the trace metal content of incremental biological tissues including bivalve shells [15, 16, 17], beluga and walrus teeth, and the pectoral fin ray of a sturgeon [18]. Evans and co-workers [19] employed LA–ICP–MS of walrus tooth cementum to investigate environmental exposure to Pb, Cu, Sr and Zn. Outridge et al. [20] (1995) reviewed the potential benefits of LA–ICP–MS analysis of temporal information embedded in hard tissues. Examples of elemental signature analysis (ESA) and the determination of lead isotope ratios in beluga whales' teeth for identification of the environmental sources by LA–ICP–MS have been discussed by Outridge [21]. Cox et al. [22] demonstrated that LA–ICP–MS could provide rapid semi-quantitative elemental information about dental tissues. In the absence of appropriate standard reference material for semi-quantification of elements in dental tissue, they studied element/element (i.e., Ca/P Ca/Mg, Ca/Na, and P/Sr) normalization as an approach for inter-sample comparison of analyte elements in the dental tissue. Major differences in mass spectral profiles of metals were observed between a human tooth from early 19th century Spitzbergen and a modern tooth from Krakow, Poland. These differences arise from the different environmental conditions that each tooth was exposed to [22]. Budd et al. [23] have shown the suitability of LA–ICP–MS to investigate elemental information from archaeological and contemporary human dentine and enamel. They obtained lead distribution line profiles across a set of contemporary and ancient teeth. The resulting lead signals were normalized to the simultaneously collected ^{46}Ca signal (least abundant isotope of a dominant matrix element). Owing to the semi-quantitative nature of their lead results, the authors used Pb/Ca ratios for comparison of lead distribution in surface enamel, core enamel, and dentine tissues within and among teeth. They found a sharp rise in lead levels in outer surface enamel (30 µm) and steadily declining lead concentrations in core enamel region, followed by moderately elevated lead concentration in the dentine tissue. They argued that core enamel and dentine is less likely to have been diagentically altered. Similarly, Lee et al. [9] investigated the prenatal and postnatal Pb, Zn, Sr, and Sn distributions in an ablated line across human and rat enamel tissues. They too used Ca (^{43}Ca) as an internal reference to normalize the elemental signal. In another study, elemental concentrations

obtained for 14 elements in a walrus tooth by ICP–AES were used as an in-house standard to estimate the semi-quantitative elemental concentrations in human teeth [24]. In a recent study, mercury diffusion in teeth cavities restored with mercury amalgam was measured by LA–ICP–MS using calcium sulfate pellets doped with analytes Hg, Ag, and Cu. Calcium-44 was used for internal standardization of analyte signals [25]. They were able to investigate the distribution of mercury and determined diffusion coefficients and lengths of mercury, silver, and copper within a tooth.

In summary, LA–ICP–MS has recently emerged as a method to solve questions that may be answered by examination of the spatial distribution of trace elements in hard tissues including human teeth. However, to date there has been very little study of the micro spatial distribution of trace elements by ICP–MS within and between dental growth layers and tissues. Thus, the purpose of this investigation is to develop a method to investigate the spatial distribution of trace metals Cu, Fe, Mg, Sr, Pb, and Zn in micro regions of a deciduous tooth encompassing the neonatal line, prenatal and postnatal enamel areas, at the dentine–enamel junction (DEJ), dentine region alone, and at the dentine–pulp junction using LA–ICP–MS.

Experimental

Tooth preparation

The exfoliated deciduous upper central incisor (Solis, Mexico catalog number 41821464) examined in this study was collected from a child living in the Solis Valley, Mexico, approximately 150 km northeast of Mexico City. The child had previously been included in a cohort that had been extensively studied from the second trimester in utero to about 6–9 months postnatal, a near perfect match of the time of calcification of this tooth. The purpose of the original study completed in the mid 1980s was to identify the functional consequence of mild-to-moderate malnutrition [26, 27]. This study, called the Nutritional Collaborative Research and Support Program on Nutritional Intake and Function (NCRSP), was funded by the United States Agency for International Development (USAID) [27]. The tooth was collected as part of a follow-up study to evaluate the consequences of nutrition and health during tooth development on the structure and chemistry of enamel (NIH R15 DEO9863). Human subjects approval was obtained from Hampshire College, USA and the National Institute of Nutrition, Mexico City, Mexico.

The tooth was cleaned with distilled deionized (DDI) water (18 MΩ cm) using a dilute nitric acid-washed toothbrush and left overnight in a plastic micro beaker (Fisher Scientific, Fairlawn, NJ, USA) containing 2% (*w*/*v*) papain solution in order to dissolve any remaining oral tissue. It was then bathed with distilled deionized water, rinsed and etched with 3% (*v*/*v*) hydrogen peroxide (30% strength, Fisher Scientific) for 30 s. Subsequently, the tooth was washed immediately with DDI water several times and dried overnight (85 °C) in an oven.

Sectioning and cleaning

The dried tooth was transferred to a plastic mold, positioned in the center, and a mixture of 4:1 epoxy resin and hardener (Buehler, Lake Bluff, IL, USA) was poured over the tooth and allowed to dry in a vacuum dissector. Once the tooth was secure in the hard resin block, it was removed from the plastic mold and longitudinally sectioned with a diamond blade on an Isomet low speed saw (Buehler, Lake Bluff, IL, USA). DDI water was used as a lubricant to minimize contamination of the tooth surface during sectioning. The resulting two halves were washed with DDI water and allowed to dry overnight.

One half-tooth section was further cut into two thin sections (~100–150 µm) for histological study of enamel structures. These sections were also used to help identify the exact location of the neonatal line because neonatal lines are not always visible in the

Table 1 Laser ablation and ICP–MS operating conditions

Laser ablation operating conditions:	
Laser type	Nd: YAG
Laser mode	Frequency quadrupled 266 nm UV, Q-switched mode
Repetition rate (Hz)	10
Laser energy (mJ)	0.85–1.02 at level 13
Number of laser shots	10
Sampling scheme	Linear raster scan
Spot size (µm)	10
Distance between lines scanning (µm)	10
Scanning speed (µm s^{-1})	20
ICP–MS operating conditions:	
Forward power (kW)	1
Ar gas flow rates (L min^{-1})	
Coolant	15
Auxiliary	1.2
Nebulizer gas	0.7–1.0
Measurement conditions:	
Dwell time (ms)	40
Resolution	high
Sweeps/reading	1
Readings/replicate	200
Replicate	1
Isotopes measured (*m*/*z*)	^{43}Ca, ^{65}Cu, ^{57}Fe, ^{25}Mg, ^{208}Pb, ^{66}Zn, and ^{88}Sr
Internal standard (*m*/*z*)	^{43}Ca

thick section to be laser ablated (Fig. 1). The surface of second half-tooth section to be laser ablated was polished smooth and etched with 1 mol L^{-1} HCl for 15 s, cleaned with acetone for 30 s, wiped, rinsed with de-ionized water, and dried before laser ablation.

Laser ablation–inductively coupled plasma-mass spectrometry (LA–ICP–MS)

A section of the tooth was inspected for developmental abnormalities and the neonatal line was located using optical microscopy (Fig. 1). A CETAC-LSX100 laser-ablation system (CETAC Technologies, Omaha, Nebraska, USA) equipped with a 266 nm Nd:YAG laser was used for laser ablation sampling of the teeth. A Perkin Elmer (PE)/Sciex Elan 6000a ICP–MS instrument (Shelton, CT, USA) was coupled to the laser ablation system for elemental analysis. Initially ICP–MS was optimized using Perkin Elmer 10 µg L^{-1} multielement tuning solution to optimize the signals for ^{24}Mg, ^{103}Rh, and ^{208}Pb. Percent oxides and doubly charged ions were less than 3%. Using these optimized liquid nebulization operating conditions as an initial benchmark, LA–ICP–MS operating conditions were later further optimized using National Institute for Standards and Technology's glass standard reference material (NIST-SRM 612). The energy level and number of laser shots were optimized by ablating the glass standard for the analyte element signals using one factor-at-a-time method. The strontium-88 signal resulting from the linear scans of the glass standard was used to optimize the lens voltage and nebulizer gas flow rate to tune the ICP–MS. This optimization work had done using Perkin Elmer, Elan-6000 optimization/tuning software. The optimized operating conditions are summarized in Table 1.

The resin block half containing the tooth section was positioned in the laser ablation chamber and the resin block was anchored on to the ablation chamber platform using double-sided 3M scotch tapes or adhesive putty. Tooth tissue micro samples were ablated on a raster scan path from the bottom right to top left of a rectangular surface area of 6.6×10^4 µm^2 (196 µm wide by 339 µm long). ^{43}Ca, ^{65}Cu, ^{57}Fe, ^{25}Mg, ^{208}Pb, ^{88}Sr, and ^{66}Zn intensities were measured in seven rectangular surface regions (A to G) of the enamel and dentine. These six regions were included because they cover both prenatal and postnatal enamel growth layers and the neonatal line, the dentine–enamel junction (DEJ), and the pulp-dentine regions (Fig. 2 and Table 2). Elemental intensity readings were taken at least 10 s before and after laser ablation to determine argon background intensity readings.

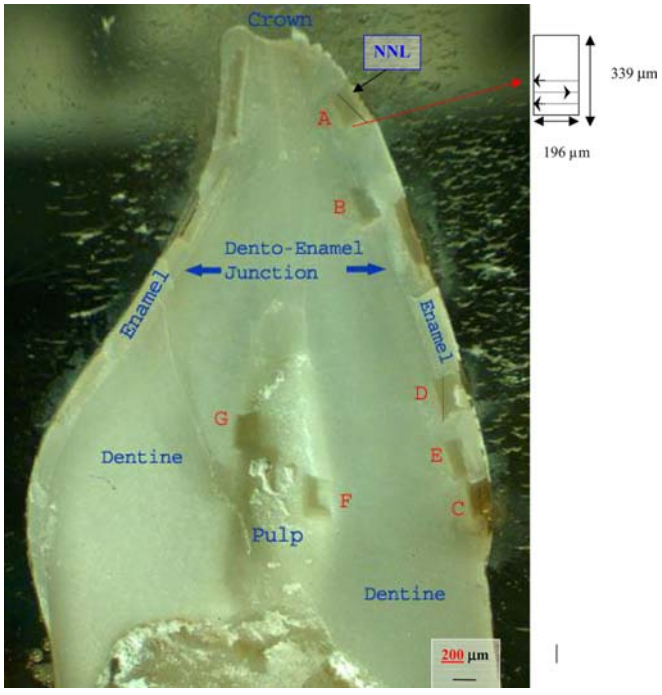

Fig. 2 Ablated regions of the deciduous incisor. *Region A*: enamel–neo natal line, *Region B*: dentine–enamel junction, *Region C*: dentine–enamel junction – surface enamel, *Region D*: dentine–enamel junction – neo natal line, *Region E*: dentine–enamel junction, *Region F*: pulp–dentine region, *Region G*: pulp–dentine

Data analyses and surface elemental distribution plotting

Rectangular surface area elemental intensity readings were obtained using the LA–ICP–MS. The LA–ICP–MS records elemental intensity readings in terms of laser run time. Those readings were imported into Microsoft Excel 2000 (Copyright 1985–1999, Microsoft Corporation, Redmond, WA, USA), and transformed into *x* and *y* coordinate position readings using laser speed, laser raster pattern, and ablated area dimensions data. Elemental signal intensities were corrected for argon background and normalized against the intensity of the ^{43}Ca signal. Normalized intensities (M/^{43}Ca) were assigned on *x* and *y* coordinates based on ablated position using a macro program written in Excel spreadsheet software.

These coordinates and normalized elemental intensity (M/^{43}Ca) data were then imported into a mapping program, Arcview GIS 3.2a, (Copyright 1992–2000, Environmental Systems Research Institute, Redlands, CA, USA – Arc View software is a geographical information system (GIS) program used by geographers, geologists and planners to show topographic and geological features or land use

Table 2 Average ^{43}Ca normalized (I ^{A}M/I ^{43}Ca)[a] elemental intensity ratios

Ablation area[c]	^{43}Ca normalized elemental intensities					
	^{66}Zn	^{208}Pb	^{25}Mg	^{57}Fe	^{88}Sr	^{65}Cu
Section A (E-NNL)	2.61±1.88[b]	1.15± 1.45	39.3± 5.7	0.10±0.11	112±18	0.01±0.02
Section B (DEJ)	2.31±1.23	0.26± 0.69	95.2±48.9	0.06±0.04	96±17	0.01±0.01
Section C (DEJ-S-E)	6.91±4.86	2.22±14.3	66.3±31.4	0.09±0.11	110±24	0.02±0.18
Section D (DEJ-NNL)	1.98±0.84	0.40± 0.87	62.0±30.4	0.06±0.03	125±19	0.01±0.02
Section E (DEJ)	2.08±0.59	0.39± 0.57	104 ±35	0.05±0.03	109±16	0.01±0.03
Section F (P-D)	10.4 ±2.3	12.8 ± 3.9	117 ±12	0.07±0.03	94±11	0.02±0.03
Section G (P-D)	12.0 ±2.5	15.4 ± 6.2	101 ±12	0.09±0.14	94±15	0.03±0.11
Overall average	5.46±4.29	4.67± 6.54	83.6±28.0	0.07±0.02	106±12	0.02±0.01

[a]I – intensity, A – mass number, M – metal
[b]±standard deviation, *n*=840 data points
[c]D – dentine, E – enamel, S – surface, P – pulp, DEJ – dentine–enamel junction, NNL – neonatal line

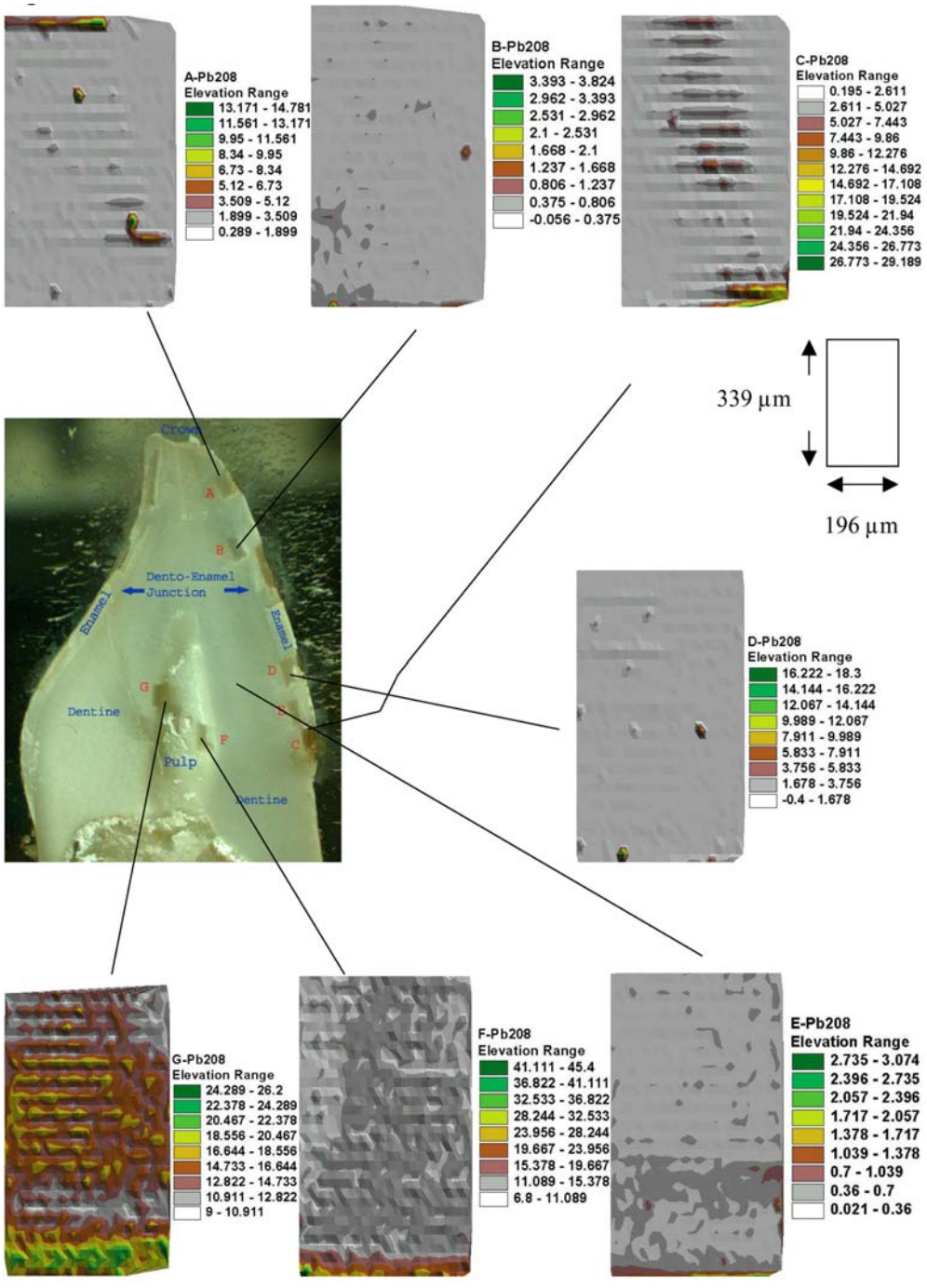

Fig. 3 Topographic maps showing micro spatial distribution of lead-208 in ablated raster areas (6.65×10^4 µm^2 or 196×339 µm^2 rectangles; details of locations are given in Fig. 2 and Table 2). ^{208}Pb intensities (cps) were normalized for ^{43}Ca. Elevations listed in the figure labels denote those normalized intensities

practices. It is a spatial analysis and visualization tool based on cell-based raster data). Using Arcview GIS's 3D Analyst extension, coordinate data points were transformed into triangular irregular networks (TIN). These TINs generated the 3D surface area maps of element intensities.

To verify the transformation from LA–ICP–MS intensity measurements to coordinate data, a raster surface area made up of white granite with the same dimensions as the tooth raster was selected for ablation. This granite had dark iron-rich deposits which had discrete visible boundaries from the rest of the white granite. The surface area map showed iron intensities three or more times greater with discrete straight boundaries that matched the location of dark deposit in the surrounding white granite.

Results and discussion

^{43}Ca normalized intensities of ^{57}Fe, ^{25}Mg, ^{208}Pb, ^{88}Sr, and ^{66}Zn were obtained from the seven ablated raster regions (339 µm×196 µm area) of the experimental tooth (Table 2). The order of magnitude of normalized elemental intensities in all tooth regions follows the general pattern Sr>Mg>>Zn>Pb>Fe>Cu. This order follows the average total elemental concentrations in dental tissue found in the scientific literature [8] except for a reversal of the order

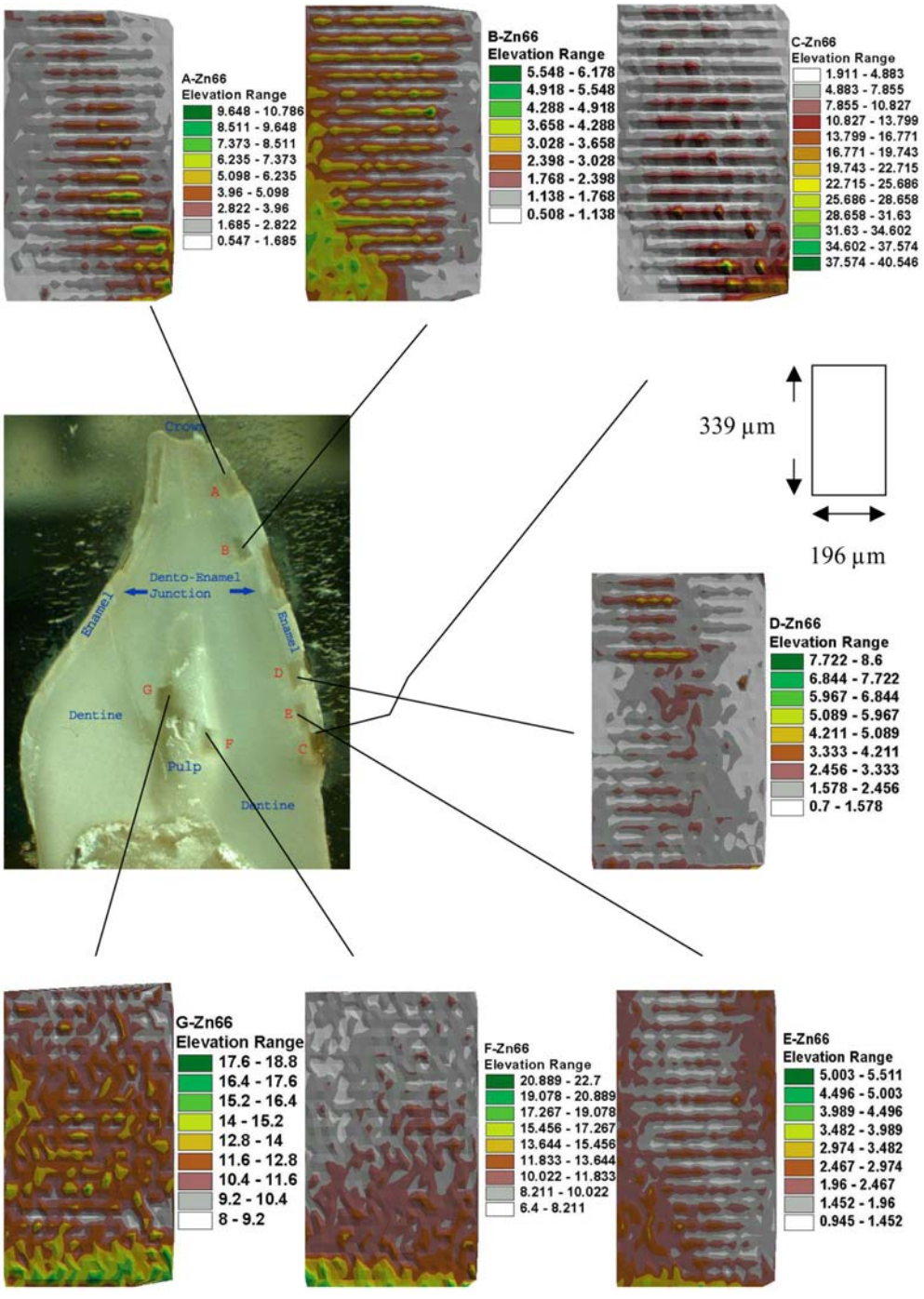

Fig. 4 Topographic maps showing micro spatial distribution of zinc-66 in ablated raster areas (6.65×10^4 µm^2 or 196×339 µm^2 rectangles; details of locations are given in Fig. 2 and Table 2). ^{66}Zn intensities (cps) were normalized for ^{43}Ca. Elevations listed in the figure labels denote those normalized intensities

for ^{88}Sr and ^{25}Mg. Average normalized intensities of ^{65}Cu, ^{25}Mg, ^{208}Pb, and ^{66}Zn in different raster regions of the tooth indicate that the magnitude of the intensities is highest in regions G and F (pulp–dentine region) (Table 2). Large variations of intensity standard deviations indicate that the elements are distributed heterogeneously in the dental tissue. Elevated zinc, lead, and copper levels were found in section C (i.e., dentine–enamel junction–surface enamel region: DEJ-S-E) as compared to Section A (i.e., enamel–neo natal line–NNL tissue area). This might be because of contributions from the outer enamel (~100 µm) region, which usually accounts for enhanced concentrations of lead [4, 23], copper, and zinc [4].

Spatial elemental distributions plotted for lead and zinc are shown in Figs. 3 and 4, respectively. Both spatial elemental distribution patterns (^{66}Zn/^{43}Ca and ^{208}Pb/^{43}Ca) in ablated raster areas (339 µm×196 µm) demonstrate great variation within regions and heterogeneous distributions of elements. Elevated normalized intensities (^{208}Pb/^{43}Caand ^{66}Zn/^{43}Ca) were observed close to the enamel surface and pulp regions.

Lead spatial distributions

Ablated region A (Fig. 3), which includes the neonatal line, shows a fairly uniform low intensity lead distribution ($^{208}Pb/^{43}Ca$ ratio ranged from 1.6–3.8) except for intense spots along the neonatal line (NNL) closer to the top left hand corner and outer enamel surface. Lead in region B, which includes the dentine–enamel junction, is evenly distributed and relatively low with the exception of a single spot. A zone of elevated lead contours can be seen along the dentine–enamel junction (DEJ) and extending toward the surface enamel. Regions D and E traverse through the DEJ and NNL, and DEJ, respectively. A homogeneously distributed zone with a few intense yet isolated spots of lead can be seen in region D, while several elevated contours are heterogeneously distributed at the bottom of the rectangle region E along with few hot spots of lead near the surface enamel present in the E region. Region F shows an increased level of lead in the dentine region versus surface enamel, which is not unusual given the fact that elevated levels of trace elements are often present in the dentine tissue. Furthermore an intense lead zone is present at the bottom half of the rectangle. Region G illustrates the most intense zone of widespread lead present in the pulp tissue. High lead concentrations at the pulp might be because of the presence of secondary dentine, which concentrates lead or residual organic matter in the pulp.

Zinc spatial distributions

The distribution of zinc (Fig. 4) is different from that of lead (Fig. 3). In some regions the intensities of zinc are 3 to 5 times greater than lead intensities described earlier (Figs. 3 and 4). Region A (Fig. 4) shows an elevated zone of Zn along the NNL line. This is an unanticipated finding that might be because of the birth process or events around birth. Elevated zones of zinc along the DEJ and low level of Zn on enamel surfaces can be seen in B and C. Region B also shows an intense zone of Zn in the lower left dentine region. The neonatal line in region D is zinc-rich and high levels of zinc are present at either side of the DEJ in the ablated area of E. Region (F) containing both dentine and pulp tissue regions, has an elevated zone of Zn at the bottom one third of the ablation region. Uniformly distributed and high zinc intensities are the norm in region G, which is located at the dental pulp. The highest intensity ratios were observed at bottom of the region.

Conclusions

We have demonstrated the potential of mapping the micro-spatial distribution of select elements in dental tissues using LA–ICP–MS. Calcium-43 served as an interference free (isobaric or polyatomic) internal standard to correct for ablation variations in the calcium rich dental tissue. The distributions of trace elements and their magnitudes can be seen in $196\times339\,\mu m^2$ raster surface maps in just the same way as a geologist examines a landscape with mountains, rivers, ridges, and forests on a topographic map or satellite picture. Similarly, these raster-ablated regions of the teeth provide unique information on trace elemental variations (in 10 μm intervals) in enamel, dentine, and pulp tissues at micro scale. These raster-ablated regions provide valuable information on trace elemental variation in enamel, dentine, and pulp. The order of magnitude of normalized elemental intensities in all tissue regions under investigation follows the general pattern Sr>Mg>>Zn>Pb>Fe>Cu. These elemental intensity topographic plots clearly illustrate elevated zinc and lead levels in the dental pulp region as compared to other tissue regions. In addition, zones of enhanced lead and zinc intensities are visible along the neonatal line. The consistency and cause of these variations should be further studied. Increased elemental intensities are also found at the areas where tissues join together. This study demonstrates that LA–ICP–MS is a sensitive microprobe technique for identification of trace elemental distributions in regions of dental tissue that calcify at different times in life. This method may provide a chronological record of variation in elemental intensities in human teeth. In addition, this methodology may be extended to investigation of other hard tissues, for example fish otolith, corals, and shells.

Acknowledgements We thank the National Science Foundation (NSF) Collaborative Research in Undergraduate Institutions (CRUI, Grant #DBI-9978793) for funding this research project. Additional financial support was obtained from the Howard Hughes Medical Institute to Hampshire College (HHMI #71100–503803) and the Kresge Foundation. We wish to acknowledge the expert laboratory assistance of Kristen Shrout and Alexis Dolphin and assistance in the field from Homero Martinez and Luzmaria Mendez, the principal investigators of the original Solis study, Adolpho Chavez, Lindsay Allen and Gretel Pelto, and finally, the openness and kindness of the study participants.

References

1. Sarnat BG, Schour IJ (1941) Am Dent Assoc 28:1989–2000
2. Fergusson JE, Purchase NG (1987) Environ Pollut 46:11–44
3. Goodman AH, Rose JC (1990) Yearb Phys Anthropol 33:59–110
4. Reitznerová E, Amarasiriwardena D, Kopčáková M, Barnes RM (2000) Fresenius J Anal Chem 367:748–754
5. Goodman AH, Dolphin AE, Amarasiriwardena DD, Klein R, Backstrand JR, Reid JB, Outridge PJ (2003) J Child Health 1: 203–214
6. Carlson SJ (1990) Vertebrate dental structures. In: Carters JG (ed) Skeletal biomineralization: patterns, processes and evolutionary trends, vol 1. Van Nostrand, New York, pp 531–556
7. Trueman CN, Tuross N (1992) Trace elements in recent and fossil bone apatite, phosphates: geochemical, geobiological and material importance. In: Kohn MJ, Rakovan J, Hughes JM (eds) Reviews in mineralogy and geochemistry, vol 48, chap 13, pp 489–521
8. Curzon MEJ, Featherstone JDB (1990) In: Lazari EP, Levy BM (eds) CRC handbook of experimental aspects of oral biochemistry. CRC Press, Boca Raton, Florida, pp 123–134
9. Lee KM, Appleton J, Cooke M, Keenan F, Sawicka-Kapusta K (1999) Anal Chim Acta 395:179–185
10. Rao GS (1984) Ann Rev Nutr 4:115–136

11. Gray AL (1985) Analyst 110:551–556
12. Moenke-Blankenburg L (1989) Laser microanalysis. Chemical analysis, vol 105. Wiley, New York
13. Darke SA, Tyson JF (1993) J Anal At Spectrom 8:145–209
14. Denoyer ER, Freedeen KJ, Hager JW (1992) Anal Chem 63: 445A–457A
15. Perkins WT, Fudge R, Pearce NJG (1991) J Anal At Spectrom 6:445–449
16. Fudge R, Palmer TJ, Pearce NGJ, Perkins WT (1993) Appl Geochem 2(Suppl):111–116
17. Bellotto VR, Mickeley N (2000) Fresenius J Anal Chem 367: 635–640
18. Evans RD, Richner P, Outridge PM (1994) J Anal At Spectrom 9:985–989
19. Evans RD, Richner P, Outridge PM (1995) Arch Environ Contam Toxicol 28:55–60
20. Outridge PM, Veinott G, Evans RD (1995) Environ Rev 3: 160–170
21. Outridge PM (1996) Spectroscopy 11:21–26
22. Cox A, Keenan F, Cooke M, Appleton J (1996) Fresenius J Anal Chem 354:254–258
23. Budd P, Montgomery J, Cox A, Krause P, Barreiro B, Thomas RG (1998) Sci Total Environ 220:121–136
24. Lochner F, Appleton J, Keenan F, Cooke M (1999) Anal Chim Acta 401:299–306
25. Hoffmann E, Stephanowitz H, Ullrich E, Skole J, Lüdke C, Hoffmann B (2000) J Anal At Spectrom 15:663–667
26. Murphy SP, Beaton GH, Calloway DH (1992) Am J Clin Nutr 56:565–572
27. Allen LH, Backstrand J, Chavez A, Pelto GH (1992) People cannot live tortillas alone: the results of the Mexico nutrition CRSP Final report to US AID, University of Connecticut